

# Anderson localization of a one-dimensional lattice model with mosaic quasi-periodic off-diagonal disorders

Yi-Cai Zhang,<sup>1,\*</sup> Rong Yuan,<sup>2</sup> and Yongjian Wang<sup>2,†</sup>

<sup>1</sup>*School of Physics and Materials Science, Guangzhou University, Guangzhou 510006, China*

<sup>2</sup>*School of Mathematical Sciences, Laboratory of Mathematics and Complex Systems, MOE, Beijing Normal University, 100875 Beijing, China*

(Dated: December 22, 2022)

In this work, we investigate Anderson localization of a one-dimensional lattice with a mosaic off-diagonal quasi-periodic hopping. It is found that the localization properties of zero-energy states depend sensitively on the parity of mosaic modulation period  $\kappa$ . If the mosaic period is an odd integer, there is no Anderson localization transition for an arbitrarily large quasiperiodic hopping. The zero-energy state is a critical state. While for an even number period and a generic quasiperiodic hopping, the zero-energy state would be a localized edge state at left (or right)-hand end of system. The above even-odd effects of mosaic period have been also transmitted into the other eigenstates near zero-energy. More specifically, when mosaic period is odd, there always exists an energy window in which the eigenstates are critical for arbitrarily strong quasiperiodic hopping. While for even period, there exists Anderson localization transition as the hopping strength increases. In addition, the Lyapunov exponent  $\gamma(E)$  and the mobility edges  $E_c$  are exactly obtained. With the Lyapunov exponent, we further find that there exist critical regions in the parameter  $\tau - E$  (for  $\kappa = 1$ ) and  $\lambda - E$  (for  $\kappa > 1$ ) plane. Furthermore, when  $E$  approaches mobility edges  $E_c$ , it is found that the critical index of localization length is  $\nu = 1$ . At the end, we show that the systems with different  $E$  can be characterized by Lyapunov exponent  $\gamma(E)$  and Avila acceleration  $\omega(E)$ .

## I. INTRODUCTION

For a conventional orthogonal class system, it is believed that an arbitrarily weakly uncorrelated diagonal disorder in one and two dimension [1] can result in the Anderson localization [2]. In three dimension, there exists mobility edge  $E_c$  which separates the localized states from extended states [3]. When the eigenenergies approach the mobility edge  $E_c$ , the localization length of localized states would diverge. Interestingly, in the presence of off-diagonal uncorrelated disorders, one-dimensional system can have a singular density of states near the zero energy [4–6], which also results in an anomalous localization [7, 8] that the localization length is proportional to the square root of system size [9–11]. If the energy deviates from zero, the eigenstates are usually localized states. If the off-diagonal disorder is correlated, the system can have localized-extended transition [12]. In the presence of both diagonal and correlated off-diagonal disorders, the one-dimensional system can also have extended states [13]. Recently, a so-called mosaic lattice model with diagonal quasiperiodic disorder has been proposed [14]. It is found that this model has mobility edges and the mobility edges can be exactly obtained with Avila's theory [15, 16].

Since there exist above anomalous properties of localizations in the model with a pure off-diagonal uncorrelated disorder, a natural question arises, how is it if there the off-diagonal hopping is quasiperiodic? One may wonder whether there exist mobility edges for off-diagonal

quasiperiodic disorder (hopping). What are the localization properties of eigenstates?

In this work, we try to answer the above questions by exploring a quasiperiodic off-diagonal disorder model with mosaic modulation. The model is

$$V_{i,i+1}\psi(i+1) + V_{i,i-1}\psi(i-1) = E\psi(i). \quad (1)$$

where

$$V_{i,i+1} = V_{i+1,i} = \begin{cases} t, & \text{for } i \neq 0 \text{ mod } \kappa \\ \frac{2\lambda \cos(2\pi\beta i + \phi)}{\sqrt{1 - \tau \cos^2(2\pi\beta i + \phi)}}, & \text{for } i = 0 \text{ mod } \kappa \end{cases} \quad (2)$$

where  $t > 0$  is constant hopping strength,  $\lambda$  describes the quasi-periodic hopping strength, positive integer  $\kappa$  is mosaic period,  $\beta$  is an irrational number, and the parameter  $\tau$  is a real number. In this work, we only consider the parameter  $\tau$  is not larger than 1, i.e.,  $\tau \leq 1$ . In addition, we should remark that there is no extended state in the above model Eq.(1). This is because by [17] (or the mechanism in [18]), the absolutely continuous spectrum which corresponds extended states is empty since there exists a sequence  $\{n_k\}$  such that  $V_{n_k, n_{k+1}} \rightarrow 0$ . Thus the mobility edges (if any) would separate localized states and critical states. In the whole paper, we take  $\beta = (\sqrt{5} - 1)/2$  and use the units of  $t = 1$  for  $\kappa > 1$  (or  $\lambda = 1$  for  $\kappa = 1$ ).

It is found that the parity of mosaic period  $\kappa$  has important influences on the localization of eigenstates near zero-energy. To be specific, if mosaic period  $\kappa$  is odd, there is no Anderson localization for arbitrarily strong hopping strength. While for even mosaic period, the system undergoes Anderson localization as the quasiperiodic hopping increases. In addition, the Lyapunov exponent

\* Corresponding author. E-mail: zhangyicai123456@163.com

† Corresponding author. E-mail: wangyongjian@amss.ac.cn

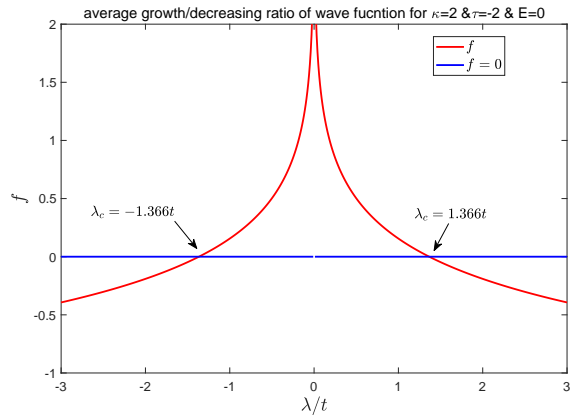


FIG. 1. The average growth/decreasing ratio of zero-energy wave function for  $\kappa = 2$ , and  $\tau = -2$ . The critical hopping strength  $\lambda = \lambda_c \simeq \pm 1.366t$  where  $f$  is exactly zero (indicated by black arrows in the figure).

$\gamma(E)$  and mobility edges are also exactly obtained with the Avila's theory. With Lyapunov exponent, we find that, some critical regions in the parameter plane would appear. In comparison with the localized states, the spatial extensions of eigenstates and their fluctuations in the critical region are much larger. Near localized-critical transition points ( $E_c$ ), the localization length diverges, i.e.,

$$\xi(E) \equiv 1/\gamma(E) \propto |E - E_c|^{-\nu} \rightarrow \infty, \text{ as } E \rightarrow E_c, \quad (3)$$

where the critical index [19]  $\nu = 1$ . Finally, we show that the systems with different parameter  $E$  can be systematically classified by Lyapunov exponent and Avila acceleration.

The work is organized as follows. First of all, we discuss the localization properties of zero-energy states for both odd and even number  $\kappa$  in Sec. II. In Sec. III, the Lyapunov exponent is calculated. Next, with the Lyapunov exponent, we determine the mobility edges and critical region in Sec. IV. In addition, Avila's acceleration is also calculated. At the end, a summary is given in Sec. V.

## II. LOCALIZATION OF ZERO-ENERGY STATE

In this section, we discuss the influences of parity of integer  $\kappa$  on the localization properties of the zero energy states. For the quasi-periodic model Eq.(1), we note that if one applies a transform  $\psi(n) \rightarrow (-1)^n \psi(n)$  in the Eq.(1), the energy would change a sign, i.e.,  $E \rightarrow -E$ . Due to the chiral (sublattice) symmetry, the energy  $E_n$  and  $-E_n$  appear in pairs [12]. In addition, the number of eigenenergies is same with the lattice site number. If the total lattice site number  $N$  is an odd number, then there would be one zero energy state at least. In the following, we find that when  $N$  is even, usually there is no

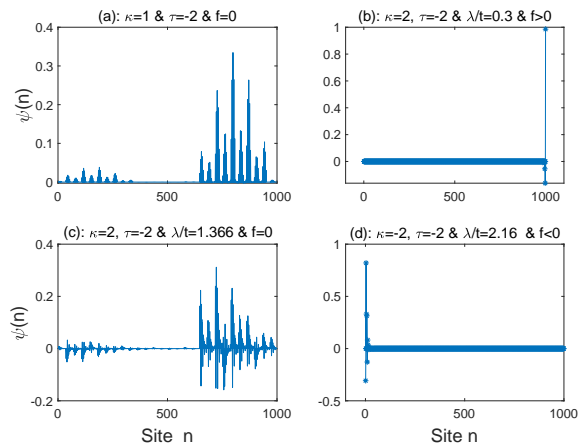


FIG. 2. Several typical zero-energy wave functions of critical states and localized edge states. Panels (a) and (c) are critical zero-energy wave functions where  $f = 0$ . Panel(b) [(d)] is localized right (left)-hand edge states where  $f > 0$  ( $f < 0$ ).

zero-energy eigenstates. In this section, we assume the total lattice number  $N$  is odd, then the zero-energy state always exists.

Furthermore, we assume the lattice sites of system are labeled with number  $i = 1, 2, 3, \dots, 2m, N = 2m+1$ , where  $m$  is a positive integer. Starting from wave functions of left-hand end site  $\psi(i = 1) = 1$  [and  $\psi(i = 0) = 0$ ], by Eq.(1), the wave function of zero-energy state can be written as

$$\begin{aligned} \psi(N = 2m + 1) &= \frac{V_{2m,2m-1}V_{2m-2,2m-3}\dots V_{4,3}V_{2,1}}{V_{2N,2N+1}V_{2m-2,2m-1}\dots V_{4,5}V_{2,3}}\psi(i = 1), \\ &= \frac{v(2m-1)v(2m-3)\dots v(3)v(1)}{v(2m)v(2m-2)\dots v(4)v(2)}. \end{aligned} \quad (4)$$

In the above equation, we set  $v(i) \equiv v(i, \phi) \equiv V_{i,i+1}$  and use the relation  $V_{i+1,i} = V_{i,i+1}$ . The average growth/decreasing ratio of wave function is

$$\begin{aligned} f &= \lim_{m \rightarrow \infty} \frac{1}{2m} \ln\left(\left|\frac{\psi(N = 2m + 1)}{\psi(i = 1)}\right|\right) \\ &= \lim_{m \rightarrow \infty} \frac{1}{2m} \ln\left(\left|\frac{v(2m-1)v(2m-3)\dots v(3)v(1)}{v(2m)v(2m-2)\dots v(4)v(2)}\right|\right). \end{aligned} \quad (5)$$

If  $f \geq 0$ ,  $f$  would be the Lyapunov exponent  $\gamma(E)$  (see Sec. III).

### A. $\kappa$ is a positive even integer

When  $\kappa$  is a positive even integer, we can assume  $N = n\kappa + 1$ , where  $n$  is an integer. Based on Eqs. (1) and (5), due to the ergodicity of the map  $\phi \rightarrow 2\pi\beta i + \phi$ , the average growth/decreasing rate of wave function can be

reduced into

$$\begin{aligned}
f &= \lim_{n \rightarrow \infty} \frac{1}{n\kappa} \ln \left( \frac{|v(\kappa-1)v(2\kappa-1)\dots v(n\kappa-1)|}{|v(\kappa)v(2\kappa)\dots v(n\kappa)|} \right), \\
&= \frac{-1}{\kappa \times 2\pi} \left[ \int_0^{2\pi} d\phi \ln(|v(\kappa, \phi)|) \right], \\
&= \frac{-1}{\kappa} \ln \left( \frac{2|\lambda/t|}{1 + \sqrt{1-\tau}} \right). \tag{6}
\end{aligned}$$

It is shown that when  $\kappa$  is a positive even integer, for a generic  $\lambda$ ,  $f$  is usually not zero. Then the zero-energy state would be localized states which may situate at right-hand edge ( $f > 0$ ) or left-hand edge ( $f < 0$ ) of the lattices (see Figs.1 and 2). So for general parameters, the zero-energy state would be a localized edge state. Only when  $f$  is exactly vanishing, i.e.,  $f = 0$ ,

$$\begin{aligned}
\rightarrow f &= \frac{-1}{\kappa} \ln \left( \frac{2|\lambda/t|}{1 + \sqrt{1-\tau}} \right) = 0 \\
\rightarrow |\lambda/t| &= |\lambda_c/t| \equiv \frac{1 + \sqrt{1-\tau}}{2}, \tag{7}
\end{aligned}$$

the zero-energy state would be a critical state (see Figs.1 and 2). The average growth/decreasing rate  $f$  for  $\kappa = 2$  and  $\tau = -2$  is reported in Fig.1. At the critical strength  $\lambda_c = \pm 1.366t$ ,  $f = 0$ . When  $\lambda$  approaches the critical  $\lambda_c$ , the localization length can be arbitrarily large, i.e.,  $\xi \equiv 1/|f| \propto 1/|\lambda - \lambda_c| \rightarrow \infty$ .

In order to investigate the properties of zero-energy states, we also numerically solve Eq.(1) for  $\kappa = 2$ ,  $\tau = -2$ , and lattice size  $N = 2 \times 500 + 1$ . Several typical wave functions for localized states and critical states are reported in Fig.2. We know that the wave function of extended state usually extends all over the whole lattices, while localized state only occupies finite lattice sites. The critical state consists of several disconnected patches which interpolates between the localized and extended states [20, 21]. From Fig.2, we see the zero energy wave function of  $f = 0$  is critical state. The wave functions with non-vanishing  $f$  correspond to localized edge states. When  $f > 0$ , the state is at right-hand end edge, while for  $f < 0$ , it is at left-hand end edge.

### B. $\kappa$ is a positive odd integer

When  $\kappa$  is a positive odd integer, we can assume  $N = 2n\kappa + 1$ , where  $n$  is an integer. Similarly,  $f$  can be written as

$$\begin{aligned}
f &= \lim_{n \rightarrow \infty} \frac{1}{2n\kappa} \ln \left( \frac{|v(\kappa)v(3\kappa)\dots v((2n-1)\kappa)|}{|v(2\kappa)v(4\kappa)\dots v(2n\kappa)|} \right), \\
&= \frac{1}{2\kappa \times 2\pi} \left[ \int_0^{2\pi} d\phi \ln(|v(\kappa, \phi)|) - \int_0^{2\pi} d\phi \ln(|v(2\kappa, \phi)|) \right], \\
&= 0. \tag{8}
\end{aligned}$$

It is shown that when  $\kappa$  is a positive odd integer, the average growth/decreasing ratio of zero-energy wave function

is exactly zero. So if  $\kappa$  is odd, all the zero-energy states are critical states.

Some interesting even-odd effects of lattice site number  $N$  have been investigated in the random off-diagonal disorder models. It is found that there exists a delocalization transition only when lattice size  $N$  is odd [22]. In addition, the localization length of the zero-energy state depends sensitively boundary conditions [23], and it can be an arbitrarily large value.

The above discussions show that the parity of integer  $\kappa$  has important influences on the localization of zero-energy states. An odd integer  $\kappa$  results in a critical zero-energy state, while an even  $\kappa$  usually gives the localized edge states (see Fig.2). We notice that the above discussion can be also applied to other forms of quasiperiodic hopping with mosaic modulations.

In the following text, we will show that the above influences of parity of  $\kappa$  are also transmitted to other eigenstates near the zero energy. To be specific, when  $\kappa$  is a positive odd integer, for a given hopping strength  $\lambda$ , the eigenstates near zero energy are always critical (see Sec.IV). So if energy is sufficiently near the zero-energy, there is no Anderson localization transition for odd  $\kappa$ . When  $\kappa$  is a positive even integer, the eigenstates near zero-energy would undergo Anderson localization transition as the quasiperiodic hopping strength increases. Then the system would have localized states near the zero-energy.

### III. THE LYAPUNOV EXPONENT

When  $E \neq 0$ , the localization properties of eigenstates can be characterized by the Lyapunov exponent. In this section, we calculate the Lyapunov exponent with the transfer matrix method [24, 25].

First of all, we assume the system is a half-infinite lattice system with left-hand end sites  $i = 0$  and  $i = 1$ . Further using Eq.(1), starting with  $\psi(0)$  and  $\psi(1)$  of left-hand end sites, the wave function can be obtained with relation

$$\Psi(i) = T(i)T(i-1)\dots T(2)T(1)\Psi(0) \tag{9}$$

where transfer matrix

$$T(n) \equiv \begin{bmatrix} \frac{E}{V_{n,n+1}} & -\frac{V_{n,n-1}}{V_{n,n+1}} \\ 1 & 0 \end{bmatrix}. \tag{10}$$

and

$$\Psi(n) \equiv \begin{bmatrix} \psi(n+1) \\ \psi(n) \end{bmatrix}. \tag{11}$$

For a given parameter  $E$ , with the increasing of  $n$ , we can assume that the wave function grows roughly according to an exponential law [26, 27], i.e.,

$$\psi(n) \sim e^{\gamma(E)n}, \text{ as } n \rightarrow \infty, \tag{12}$$

where  $\gamma(E) \geq 0$  is Lyapunov exponent which measures the average growth rate of wave function. If the parameter  $E$  is not an eigen-energy of  $H$ , the Lyapunov exponent would be positive, i.e.,  $\gamma(E) > 0$  [28]. When  $E$  is an eigen-energy of system, the Lyapunov exponent can be zero or positive [21]. For critical states, the Lyapunov exponent  $\gamma(E) \equiv 0$ . While for localized states, the Lyapunov exponent  $\gamma(E) > 0$ .

Consequently the Lyapunov exponent can be written as

$$\begin{aligned} \gamma(E) &= \lim_{L \rightarrow \infty} \frac{\log(|\Psi(L)|/|\Psi(0)|)}{L} \\ &= \lim_{L \rightarrow \infty} \frac{\log(|T(L)T(L-1)\dots T(2)T(1)\Psi(0)|/|\Psi(0)|)}{L} \end{aligned} \quad (13)$$

where  $L$  is a positive integer and

$$|\Psi(n)| = \sqrt{|\psi(n+1)|^2 + |\psi(n)|^2}. \quad (14)$$

In the following, we view the adjacent  $\kappa$  lattice sites as a ‘‘super unit cell’’. Next we assume  $L = m\kappa + 1$  ( $m$  is an integer) and  $|\Psi(0)|/|\Psi(1)|$  is a finite non-zero real number, the Lyapunov exponent can be reduced into

$$\begin{aligned} \gamma(E) &= \lim_{L \rightarrow \infty} \frac{\log(|\Psi(L)|/|\Psi(0)|)}{m\kappa + 1} \\ &= \lim_{m \rightarrow \infty} \frac{\log(|T(m\kappa + 1)T(m\kappa)\dots T(2)\Psi(1)|/|\Psi(0)|)}{m\kappa} \\ &= \lim_{m \rightarrow \infty} \frac{\log(|T(m\kappa + 1)T(m\kappa)\dots T(2)\Psi(0)|/|\Psi(0)|)}{m\kappa} \\ &= \frac{1}{\kappa} \lim_{m \rightarrow \infty} \frac{\log(|CT_m.CT(m-1)\dots CT_1\Psi(0)|/|\Psi(0)|)}{m} \end{aligned} \quad (15)$$

where cluster transfer matrix  $CT_n$  for  $n$ -th ‘‘super unit cell’’ is defined as

$$\begin{aligned} CT_n &\equiv T(n\kappa + 1)T(n\kappa)\dots T((n-1)\kappa + 3)T((n-1)\kappa + 2) \\ &= \begin{bmatrix} E & -v(n\kappa) \\ 1 & 0 \end{bmatrix} \begin{bmatrix} \frac{E}{v(n\kappa)} & -\frac{1}{v(n\kappa)} \\ 1 & 0 \end{bmatrix} \begin{bmatrix} E & -1 \\ 1 & 0 \end{bmatrix}^{\kappa-2} \\ &= \frac{\begin{bmatrix} E^2 - (E^2\tau + 4\lambda^2)\cos^2(\theta_n) & -E(1 - \tau\cos^2(\theta_n)) \\ E(1 - \tau\cos^2(\theta_n)) & -1 + \tau\cos^2(\theta_n) \end{bmatrix}}{2\lambda\cos(\theta_n)\sqrt{1 - \tau\cos^2(\theta_n)}} \\ &\times \begin{bmatrix} E & -1 \\ 1 & 0 \end{bmatrix}^{\kappa-2} \end{aligned} \quad (16)$$

where  $\theta_n = 2\pi\beta n\kappa + \phi$ .

The cluster transfer matrix Eq.(16) can be further written as a product of two parts, i.e.,  $CT_n = A_n B_n$ , where

$$\begin{aligned} A_n &= \frac{1}{2\lambda\cos(\theta_n)\sqrt{1 - \tau\cos^2(\theta_n)}}, \\ B_n &= \begin{bmatrix} B_{11} & B_{12} \\ B_{21} & B_{22} \end{bmatrix} \begin{bmatrix} E & -1 \\ 1 & 0 \end{bmatrix}^{\kappa-2}, \end{aligned} \quad (17)$$

with  $B_{11} = E^2 - (E^2\tau + 4\lambda^2)\cos^2(\theta_n)$ ,  $B_{21} = -B_{12} = E(1 - \tau\cos^2(\theta_n))$  and  $B_{22} = -1 + \tau\cos^2(\theta_n)$ . Now the Lyapunov exponent is

$$\gamma(E) = \frac{1}{\kappa} [\gamma_A(E) + \gamma_B(E)], \quad (18)$$

where

$$\gamma_A(E) = \lim_{m \rightarrow \infty} \frac{\log(|A(m)A(m-1)\dots A(2)A(1)|)}{m}. \quad (19)$$

and  $\gamma_B(E)$  are given by

$$\gamma_B(E) = \lim_{m \rightarrow \infty} \frac{\log(|B(m)B(m-1)\dots B(2)B(1)\Psi(0)|/|\Psi(0)|)}{m}. \quad (20)$$

In the following, we would use Avila’s global theory [15] to get the Lyapunov exponent and the Avila’s acceleration (see next section). Following Refs.[16, 29], first of all, we complexify the phase  $\phi \rightarrow \phi + i\epsilon$  with  $\epsilon > 0$ , e.g.,  $A_n = \frac{1}{2\lambda\cos(2\pi\beta n\kappa + \phi + i\epsilon)\sqrt{1 - \tau\cos^2(2\pi\beta n\kappa + \phi + i\epsilon)}}$ . In addition, due to the ergodicity of the map  $\phi \rightarrow 2\pi\beta n + \phi$ , we can write  $\gamma_A(E)$  as an integral over phase  $\phi$  [30], consequently

$$\begin{aligned} \gamma_A(E, \epsilon) &= \frac{1}{2\pi} \int_0^{2\pi} d\phi \ln\left(\left|\frac{1}{2\lambda\cos(\phi + i\epsilon)\sqrt{1 - \tau\cos^2(\phi + i\epsilon)}}\right|\right) \\ &= -\epsilon + \ln\left(\left|\frac{2}{\lambda(1 + \sqrt{1 - \tau})}\right|\right), \end{aligned} \quad (21)$$

for  $\epsilon < \ln\left|\frac{2+2\sqrt{1-\tau}-\tau}{\tau}\right|$ .

Next we take  $\epsilon \rightarrow 0$

$$\begin{aligned} B_n &= \frac{e^{-i(4\pi\beta n\kappa + \phi) + 2\epsilon}}{4} \begin{bmatrix} -(E^2\tau + 4\lambda^2) & E\tau \\ -E\tau & \tau \end{bmatrix} \begin{bmatrix} E & -1 \\ 1 & 0 \end{bmatrix}^{\kappa-2} \\ &+ O(1). \end{aligned} \quad (22)$$

Then for large  $\epsilon$ , i.e.,  $\epsilon \gg 1$ ,  $\gamma_B(E, \epsilon)$  is determined by the largest eigenvalue (in absolute value) of  $B_n$ , i.e.,

$$\gamma_B(E, \epsilon) = 2\epsilon + \ln\left(\left|\frac{|P| + \sqrt{P^2 + 16\lambda^2\tau}}{8}\right|\right), \quad (23)$$

where

$$P = (\tau E^2 + 4\lambda^2)a_\kappa + \tau a_{\kappa-2} - 2\tau E a_{\kappa-1}. \quad (24)$$

and  $a_\kappa$ , is given by

$$a_\kappa = \frac{1}{\sqrt{E^2 - 4}} \left[ \left(\frac{E + \sqrt{E^2 - 4}}{2}\right)^{\kappa-1} - \left(\frac{E - \sqrt{E^2 - 4}}{2}\right)^{\kappa-1} \right]. \quad (25)$$

When  $\epsilon$  is very small, using the facts that  $\gamma(E, \epsilon) \geq 0$  and  $\gamma_B(E, \epsilon)$  is a convex and piecewise linear function of  $\epsilon$  [15, 29], one can get

$$\begin{aligned} \gamma(E, \epsilon) &= \text{Max}\{0, \gamma_A(E, \epsilon) + \gamma_B(E, \epsilon)\}, \\ &= \frac{1}{\kappa} \text{Max}\{0, \epsilon + \ln\left(\left|\frac{|P| + \sqrt{P^2 + 16\lambda^2\tau}}{4\lambda(1 + \sqrt{1 - \tau})}\right|\right)\} \end{aligned} \quad (26)$$

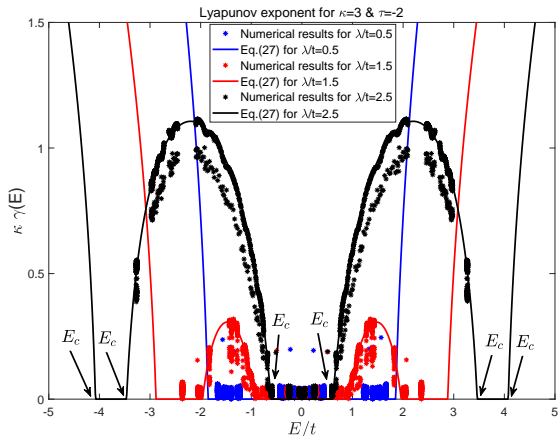


FIG. 3. Lyapunov exponents for  $\kappa = 3$ ,  $\tau = -2$ , and  $\lambda/t = 0.5, 1.5, 2.5$ . The discrete points are the numerical results for all the eigenenergies. The solid lines are given by Eq.(27). The mobility edges for  $\lambda/t = 2.5$  are indicated by black arrows. Near mobility edges of the localized-critical transition, the Lyapunov exponent  $\gamma(E) \propto |E - E_c|$  approaches zero (as  $E \rightarrow E_c$ ). The critical index of the localization length  $\nu = 1$ .

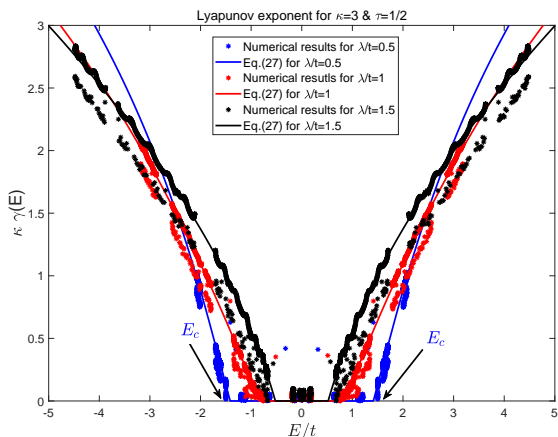


FIG. 4. Lyapunov exponents for  $\kappa = 3$  and  $\tau = 1/2$ , and  $\lambda/t = 0.5, 1.0, 1.5$ . The discrete points are the numerical results for all the eigenenergies. The solid lines are given by Eq.(27). The mobility edges for  $\lambda/t = 0.5$  are indicated by black arrows. Near mobility edges of the localized-critical transition (e.g.,  $E_c/t \simeq \pm\sqrt{2}$  for  $\lambda/t = 0.5$ ), the Lyapunov exponent  $\gamma(E) \propto |E - E_c|$  approaches zero (as  $E \rightarrow E_c$ ). The critical index of the localization length  $\nu = 1$ .

Furthermore, when  $\epsilon = 0$ , the Lyapunov exponent  $\gamma(E) \equiv \gamma(E, \epsilon = 0)$  is

$$\gamma(E) = \frac{1}{\kappa} \text{Max}\{\ln \left| \frac{|P(E)| + \sqrt{P^2(E) + 16\lambda^2\tau}}{4\lambda(1 + \sqrt{1 - \tau})} \right|, 0\} \quad (27)$$

where

$$P(E) = (\tau E^2 + 4\lambda^2)a_\kappa + \tau a_{\kappa-2} - 2\tau E a_{\kappa-1} \quad (28)$$

and

$$a_\kappa = \frac{1}{\sqrt{E^2 - 4}} \left[ \left( \frac{E + \sqrt{E^2 - 4}}{2} \right)^{\kappa-1} - \left( \frac{E - \sqrt{E^2 - 4}}{2} \right)^{\kappa-1} \right]. \quad (29)$$

When  $\tau = 0$ , then  $P(E) = 4\lambda^2 a_\kappa$ , and

$$\gamma(E) = \frac{1}{\kappa} \text{Max}\{\ln |\lambda a_\kappa|, 0\}. \quad (30)$$

The above formula Eq.(27) has been verified by our numerical results (see Figs.3 and 4). In our numerical calculations, in order to get the correct Lyapunov exponents, on the one hand, the integer  $L$  should be sufficiently large. On the other hand,  $L$  should be also much smaller than the system size  $N$ , i.e.,  $1 \ll L \ll N$ .

To be specific, taking  $\kappa = 3$ ,  $\tau = -2, 1/2$ , system size  $N = 3 \times 1000$ , we get the  $N = 3 \times 1000$  eigenenergies and eigenstates. Then we calculate the Lyapunov exponents numerically for all the eigenenergies [see the several sets of discrete points in Figs.3 and 4]. In our numerical calculation, we take  $L = 200$ , phase  $\phi = 0$ ,  $\psi(0) = 0$  and  $\psi(1) = 1$  in Eq.(13). The solid lines of Figs.3 and 4 are given by Eq.(27) with same parameters. It is shown that most of all discrete points fall onto the solid lines.

However, we also note that there are some discrete points of localized states which are not on the solid lines. This is because these localized wave functions are too near the left-hand boundary of system.

#### IV. MOBILITY EDGE AND CRITICAL REGION

In this section, based on the Lyapunov exponent formula Eq.(27), we determine the mobility edges and the critical region. By the Eq.(27), the mobility edges  $E_c$  which separate the localized states from the critical states, is determined by

$$\gamma(E = E_c) = \frac{1}{\kappa} \ln \left| \frac{|P(E)| + \sqrt{P^2(E) + 16\lambda^2\tau}}{4\lambda(1 + \sqrt{1 - \tau})} \right| = 0 \quad (31)$$

then

$$|P(E = E_c)| = 4|\lambda|\sqrt{1 - \tau}, \quad (32)$$

The critical regions which consist of critical states is given by

$$|P(E)| < 4|\lambda|\sqrt{1 - \tau}. \quad (33)$$

By expanding the Lyapunov exponent near the mobility edges  $E_c$ , we get

$$\gamma(E) \propto |E - E_c| \rightarrow 0, \text{ as } E \rightarrow E_c. \quad (34)$$

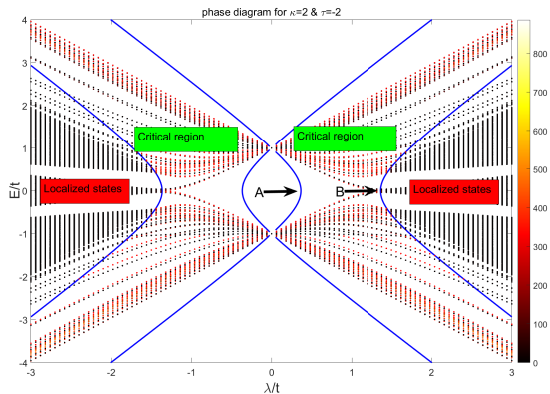


FIG. 5. Phase diagram in  $(\lambda, E)$  plane for  $\kappa = 2$  and  $\tau = -2$ . When  $E$  is near zero, there exists localized-critical transitions. The blue solid lines are the phase boundaries (mobility edges  $E_c$ ), which are given by Eq.(32). Standard deviations are represented with different colors.

Then the localization length is

$$\xi(E) \equiv 1/\gamma(E) \propto |E - E_c|^{-1} \rightarrow \infty, \text{ as } E \rightarrow E_c. \quad (35)$$

Its critical index is 1 [see the finite slopes of solid lines near  $E_c$  in Figs.3 and 4].

In order to further distinguish the localized states from the critical states, we also numerically calculate standard deviation of coordinates of eigenstates [31]

$$\sigma = \sqrt{\sum_i (i - \bar{i})^2 |\psi(i)|^2}, \quad (36)$$

where the average value of coordinate  $\bar{i}$  is

$$\bar{i} = \sum_i i |\psi(i)|^2. \quad (37)$$

The standard deviation  $\sigma$  describes the spatial extension of wave function in the lattices. The phase diagram in  $[\lambda(\tau) - E]$  plane is reported in Figs.5,6,7 and 8. In Figs.5,6,7 and 8, the standard deviations of coordinates are represented with different colors. From Figs.5,6,7 and 8, we can see that when the states are localized, standard deviations of coordinates are very small. For critical states, the standard deviations are very large.

From Figs. 5, 7, and 8, we see that when  $\kappa > 1$ , there are  $\kappa - 1$  loops for small hopping strength  $\lambda/t$  in the phase diagram. Within the loops, the Lyapunov exponent is positive, i.e.,  $\gamma(E) > 0$ . Then if there is some eigenstates in the loops, these states would be localized states. However, numerical results show that there are no eigenenergies fall into the loops.

When  $\lambda/t = 0$ , we see the system has  $\kappa$  eigenenergies with multitude degeneracies. This is because when  $\lambda/t = 0$ , the system in fact is composed by a lot of identical independent unit cells with  $\kappa$  lattice sites. Within

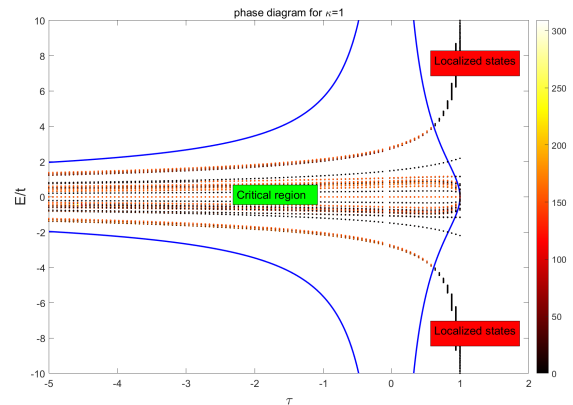


FIG. 6. Phase diagram for  $\kappa = 1$ . When energy is near zero-energy, the states are always critical states with vanishing Lyapunov exponent.

a unit cell, there are exactly  $\kappa$  eigenenergies. With the increasing of  $\lambda/t$ , the degeneracies are removed and the system enters into the critical regions. In addition, we also find that the parity of  $\kappa$  also has important effects on the phase diagram.

#### A. $\kappa$ is an even number

When  $\kappa$  is even number and the energy  $E$  is very near zero, there exist Anderson localizations if potential hopping strength  $\lambda$  is sufficiently large (see Fig.5 for  $\kappa = 2$ ). Especially when  $E \rightarrow 0$ , we get two critical hopping strengths

$$\lambda_{c1} = \pm \frac{1 - \sqrt{1 - \tau}}{2} \quad \& \quad \lambda_{c2} = \pm \frac{1 + \sqrt{1 - \tau}}{2}, \quad (38)$$

which are independent of the  $\kappa$ . Here  $\lambda_{c1}$  ( $\lambda_{c2}$ ) corresponds the point A (B) in Fig.5. It is noticed that  $\lambda_{c2}$  coincides the critical  $\lambda_c$  in Sec.II, where the average growth rate of zero-energy wave function is zero.

From Fig.5, we can see that when the hopping  $\lambda$  is in the interval  $|\lambda_{c1}| < \lambda < |\lambda_{c2}|$ , the eigenstates are critical states. Outside the interval, the eigenstates become localized states. So there exist Anderson localization transitions for even  $\kappa$ .

#### B. $\kappa$ is an odd number

When  $\kappa = 1$ , the system has no the energy scale  $t$ , then we would use the units of  $\lambda = 1$ . In Fig.6, we report the phase diagram of the  $\tau - E$  plane. From Fig.6, we see if  $\tau < 0$ , all the eigenstates are in the critical region. Only when  $\tau$  is positive and sufficiently large, the system has localized states. When  $\tau$  gets nearer

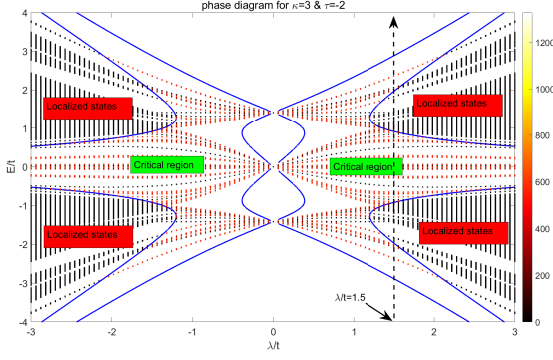


FIG. 7. Phase diagram in  $(\lambda, E)$  plane for  $\kappa = 3$  and  $\tau = -2$ . When  $E$  is near zero, there are no localized-critical transitions. The blue solid lines are the phase boundaries (mobility edges  $E_c$ ), which are given by Eq.(32). Standard deviations are represented with different colors.

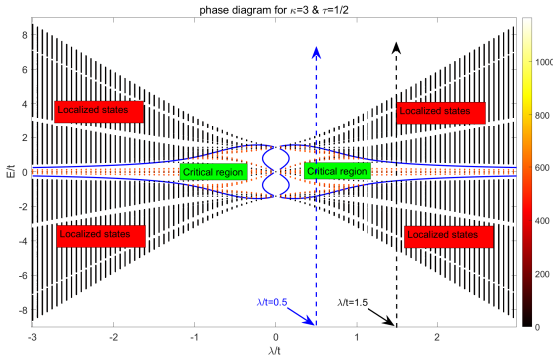


FIG. 8. Phase diagram in  $(\lambda, E)$  plane for  $\kappa = 3$  and  $\tau = 1/2$ . There exists localized-critical transitions for nonzero energy states. The blue solid lines are the phase boundaries (mobility edges  $E_c$ ), which are given by Eq.(32). Standard deviations are represented with different colors.

and nearer to 1, i.e.,  $\tau \rightarrow 1^-$ , the range of energy spectrum becomes larger and larger, and eventually diverges. This is because when  $\tau = 1$ , the Hamiltonian defined by the Eq.(1) would be an unbounded operator, e.g.,  $\frac{2\lambda \cos(2\pi\beta i + \phi)}{\sqrt{1 - \tau \cos^2(2\pi\beta i + \phi)}} = \frac{2\lambda \cos(2\pi\beta i + \phi)}{|\sin(2\pi\beta i + \phi)|}$  diverges for some lattice site index  $i$ .

When  $\kappa > 1$  and the energy  $E$  is very near zero, there are no Anderson localizations for a given potential strength  $\lambda$  (see Figs.7, and 8). If  $\lambda$  is very large, i.e.,  $\lambda \rightarrow \pm\infty$ , the mobility edge can be obtained by Eq.(32), i.e.,

$$E_c = \pm \frac{2\sqrt{1-\tau}}{(\kappa-1)|\lambda|}, \text{ as } \lambda \rightarrow \pm\infty. \quad (39)$$

It is shown that for an arbitrarily strong quasiperiodic hopping strength  $\lambda$ , there always exists an energy win-

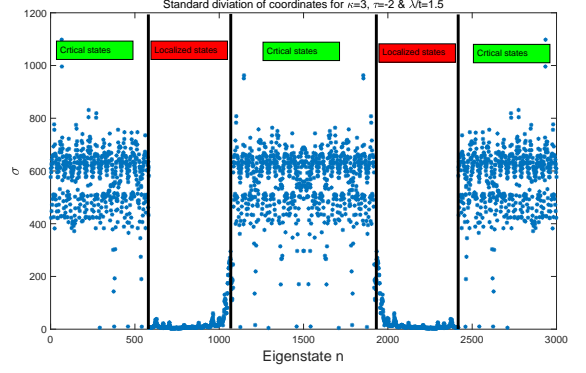


FIG. 9. Standard deviations of localized states and critical states for parameters  $\kappa = 3$ ,  $\tau = -2$  and  $\lambda/t = 1.5$ . The eigenenergy  $E_n$  increases gradually as eigenstate index  $n$  runs from 1 to 3000 (along the black dashed line of Fig.7).

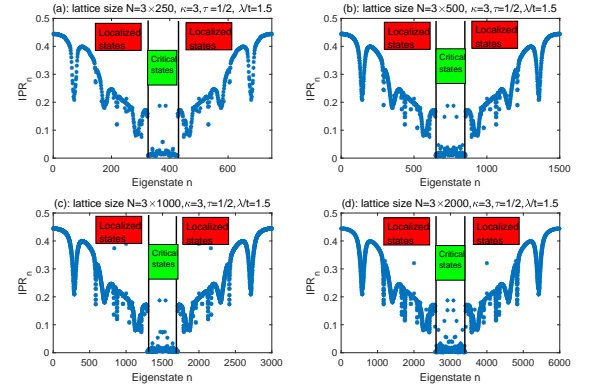


FIG. 10. The inverse participation ratio  $IPR_n$  of all the eigenstates for system size  $N = 3 \times 250, 3 \times 500, 3 \times 1000$  and  $N = 3 \times 2000$ . The eigenenergy  $E_n$  increases gradually as eigenstate index  $n$  runs from 1 to  $N$  (along the black dashed line of Fig.8).

dow, i.e.,  $-\frac{2\sqrt{1-\tau}}{(\kappa-1)|\lambda|} < E < \frac{2\sqrt{1-\tau}}{(\kappa-1)|\lambda|}$ , in which there exist critical states. With the increasing of  $\lambda$ , the energy window of critical regions gets smaller and smaller.

For given parameters  $\kappa = 3$ ,  $\tau = -2$ ,  $\lambda/t = 1.5$ , we report the standard deviations of all the eigenstates in Fig.9. It is shown that in comparison with localized states, the critical states have much larger fluctuation of standard deviations.

In order to investigate the properties of the wave functions of critical states, we also numerically calculate the inverse participation ratio  $IPR_n$  of all eigenstates for different system sizes  $N = 3 \times 250, 3 \times 500, 3 \times 1000$  and  $N = 3 \times 2000$  [32, 33], i.e.,

$$IPR_n = \sum_i |\psi_n(i)|^4. \quad (40)$$

where  $\psi_n(i)$  is the normalized wave function for  $n$ -th



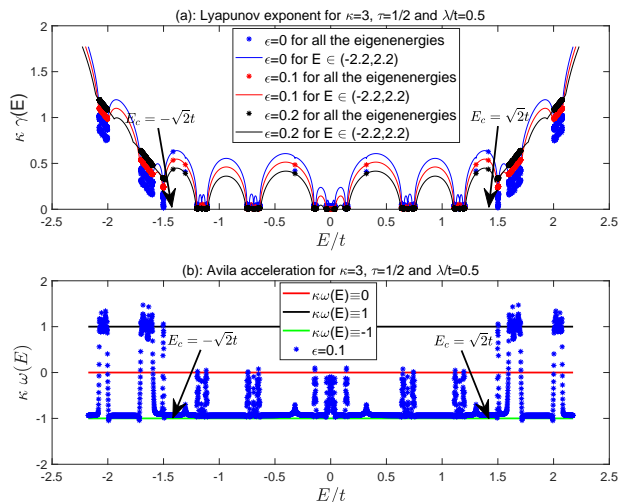


FIG. 11. Lyapunov exponents and Avila's accelerations. (a): Lyapunov exponents for  $\kappa = 3$ ,  $\tau = 1/2$  and  $\lambda/t = 0.5$  (along the blue dashed line of Fig.8). (b): Avila's acceleration for for  $\kappa = 3$ ,  $\tau = 1/2$  and  $\lambda/t = 0.5$ . The mobility edges  $E_c = \pm\sqrt{2}t$  are indicated by black arrows.

eigenstate. The results are reported in Fig.10. We find that the IPRs of localized states are basically same for different system sizes  $N$ , while the IPRs of critical states have much larger fluctuation.

On the whole, the IPR of critical states decreases with the increasing of system size  $N$ . The decreasing law can be captured by a function

$$\overline{IPR} \propto 1/N^x, \quad (41)$$

where  $\overline{IPR}$  is an average value of the  $IPR$  within a typical energy interval. It is believed that, for localized states, the scaling exponent  $x = 0$ . While for extended states (like plane wave states), the scaling exponent  $x = 1$ . For critical states, the exponent should be  $0 < x < 1$ . For different system sizes  $N$ , due to randomness of  $IPR$  of critical states (see Fig.10), it is difficult to get a definite scaling exponent  $x$ . Here we find that for the critical states in the energy interval  $-0.12 < E/t < 0.12$ , its average value  $\bar{x} \simeq 0.47$ .

### C. Avila acceleration

In addition, for the bounded quasi-periodic potentials, Avila also defined the acceleration  $\omega(E)$  by [15]

$$\kappa\omega(E) = \lim_{\epsilon \rightarrow 0^+} \frac{\gamma(E, \epsilon) - \gamma(E, 0)}{\epsilon}. \quad (42)$$

Using Eqs.(26), when real number  $E$  is an eigenvalue, we get the Avila acceleration

$$\kappa\omega(E) = \begin{cases} 1, & \text{for energy of localized state} \\ 0, & \text{for energy of critical state} \end{cases} \quad (43)$$

The above results are verified by our numerical calculations [see Fig.11]. To be specific, taking  $\tau = 1/2$ ,  $\lambda/t = 0.5$  and  $\epsilon = 0, 0.1, 0.2$ , we calculate the Lyapunov exponents with Eq.(13) (taking the complexified phase  $\phi \rightarrow \phi + i\epsilon = i\epsilon$ ) for interval  $-2.2 \leq E \leq 2.2$  [see the three solid lines in panel (a) of Fig.11]. In our calculation, we take  $L = 200$ ,  $\psi(0) = 0$  and  $\psi(1) = 1$  in Eq.(13). At the same time, we calculate the Lyapunov exponents for all the eigenenergies with same parameters [see the three sets of discrete points in panel (a) of Fig.11]. We can find that if  $E$  is an eigenenergy of critical state [ $\gamma(E) = 0$ ], the Lyapunov exponents are the same for all three different  $\epsilon = 0, 0.1, 0.2$ . While when  $E$  is an eigenenergy of localized state [ $\gamma(E) > 0$ ], the Lyapunov exponents are different for three different  $\epsilon = 0, 0.1, 0.2$ . Their differences are linearly proportional to  $\Delta\epsilon = 0.1$  in Fig. 11.

By taking  $\epsilon = 0.1$ , we also approximately calculate the Avila's acceleration  $\omega(E)$  by

$$\kappa\omega(E) \simeq \frac{\gamma(E, \epsilon) - \gamma(E, 0)}{\epsilon}, \quad (44)$$

[see panel (b) of Fig.11]. It shows that when  $E$  is an eigenenergy of localized state [ $\gamma(E) > 0$ ], the Avila's acceleration is 1. When  $E$  is an eigenenergy of critical state [ $\gamma(E) = 0$ ], the Avila's acceleration is 0. We also notice that if  $E$  is not an eigenvalue, the Avila's acceleration is  $-1$ .

Further combining Eq.(27) and Eq.(43), then one can classify systems with different real parameter  $E$  (different phases) by Lyapunov exponent and the quantized acceleration, i.e.,

$$\begin{aligned} (a) : & \gamma(E) > 0 \ \& \ \kappa\omega(E) = -1, \ \text{if } E \text{ is not an eigenvalue} \\ (b) : & \gamma(E) > 0 \ \& \ \kappa\omega(E) = 1, \ \text{for localized state} \\ (c) : & \gamma(E) = 0 \ \& \ \kappa\omega(E) = 0, \ \text{for critical state.} \end{aligned} \quad (45)$$

## V. SUMMARY

In conclusion, we investigate the localization properties of the one-dimensional lattice model with off-diagonal mosaic quasiperiodic hopping. The parity of mosaic periodic has important effects on the localization of zero-energy states. When the mosaic period is odd, there always exists an energy window for critical states regardless hopping strength. While for even period, the states near zero-energy would become localized edge states for a sufficiently large hopping strength. It is found that there exist mobility edges which separate the localized states from critical states. Within the critical region, the spatial extensions of eigenstates have large fluctuation.



The Lyapunov exponents and mobility edges are exactly obtained with Avila's theory. Furthermore, it is found that the critical index of localization length  $\nu = 1$ . For  $\kappa = 3$  and  $\tau = 1/2$ , the numerical results show that the scaling exponent of inverse participation ratio (IPR) of critical states  $x \simeq 0.47$ . It is shown that these states indeed are critical states. In addition, it is shown that the Lyapunov exponent and Avila's acceleration can be used to classify the systems with different  $E$ .

## ACKNOWLEDGEMENTS

This work was supported by the NSFC under Grants Nos. 11874127, 12061031, 12171039, 11871007, the Joint Fund with Guangzhou Municipality under No. 202201020137, and the Starting Research Fund from Guangzhou University under Grant No. RQ 2020083.

- 
- [1] E. N. Economou, *Green's Functions in Quantum Physics*, (Springer-Verlag Berlin Heidelberg, Third Edition, 2006).
- [2] P. W. Anderson, Absence of Diffusion in Certain Random Lattices, *Phys. Rev.* **109**, 1492 (1957).
- [3] E. N. Economou and Morrel H. Cohen, Existence of Mobility Edges in Anderson's Model for Random Lattices, *Phys. Rev.* **5**, 2931 (1972).
- [4] F. Dyson, The dynamics of a disordered linear chain, *Phys. Rev.* **92**, 1331 (1953).
- [5] Leon Balents and Matthew P. A. Fisher, Delocalization transition via supersymmetry in one dimension, *Phys. Rev. B* **56**, 12907 (1997).
- [6] T. P. Eggarter and R. Riedinger, Singular behavior of tight-binding chains with off-diagonal disorder, *Phys. Rev. B* **18**, 569 (1978).
- [7] George Theodorou and Morrel H. Cohen, Extended states in a one-dimensional system with off-diagonal disorder, *Phys. Rev. B* **13**, 4597 (1976).
- [8] P. D. Antoaiou, E. N. Eeonomout, Absence of Anderson's transition in random lattices with off-diagonal disorders, *Phys. Rev. B* **16**, 3768 (1977).
- [9] M. Intui and S. A. Trugman, Unusual properties of mid-band states in systems with off-diagonal disorder , *Phys. Rev. B* **49**, 3190 (1992).
- [10] L Fleishman and D C Licciardello 1977 *J. Phys. C: Solid State Phys.* **10** L125
- [11] F.M. Izrailev, A.A. Krokhnin, and N.M. Makarov, Anomalous localization in low-dimensional systems with correlated disorder *Physics Reports* **512** (2012) 125-254.
- [12] H. Cheraghchi, S. M. Fazeli, and K. Esfarjani, Localization-delocalization transition in a one-dimensional system with long-range correlated off-diagonal disorder, *Phys. Rev. B* **72**, 174207 (2005).
- [13] Wei Zhang and Sergio E. Ulloa, Extended states in disordered systems: Role of off-diagonal correlations, *Phys. Rev. B* **69**, 153203 (2004).
- [14] Yucheng Wang, Xu Xia, Long Zhang, Hepeng Yao, Shu Chen, Jiangong You, Qi Zhou, and Xiong-Jun Liu, One-Dimensional Quasiperiodic Mosaic Lattice with Exact Mobility Edges, *Phys. Rev. Lett.* **125**, 196604 (2020).
- [15] Artur Avila, Global theory of one-frequency Schrödinger operators, *Acta Math.*, **215** (2015), 1-54.
- [16] Yucheng Wang, Xu Xia, Yongjian Wang, Zuohuan Zheng, and Xiong-Jun Liu, Duality between two generalized Aubry-André models with exact mobility edges, *Phys. Rev. B* **103**, 174205 (2021).
- [17] Simon Barry and Thomas Spencer, Trace class perturbations and the absence of absolutely continuous spectra, *Commun. Math.Phys.*, 1989, **125**: 113-125.
- [18] Xin-Chi Zhou, Yongjian Wang, Ting-Fung Jeffrey Poon, Qi Zhou, and Xiong-Jun Liu, Exact new mobility edges between critical and localized states, in preparation (2022).
- [19] Bodo Huckestein and Bernhard Kramer, One-Parameter Scaling in the Lowest Landau Band: Precise Determination of the Critical Behavior of the Localization Length, *Phys. Rev. Lett.* **64**, 1437 (1990).
- [20] T. Liu, X. Xia, S. Longhi, and L. Sanchez-Palencia, Anomalous mobility edges in one-dimensional quasiperiodic models, *SciPost Phys.* **12**, 27 (2022).
- [21] Yi-Cai Zhang, and Yan-Yang Zhang, Lyapunov exponent, mobility edges, and critical region in the generalized Aubry-André model with an unbounded quasiperiodic potential, *Phys. Rev. B* **105**, 174206 (2022).
- [22] P. W. Brouwer, C. Mudry, B. D. Simons, and A. Altland, Delocalization in Coupled One-Dimensional Chains , *Phys. Rev. Lett.* **81**, 862 (1998).
- [23] P. W. Brouwer, A. Furusaki, Y. Hatsugai, Y. Morita, and C. Mudry, Zero modes in the random hopping model , *Phys. Rev. B* **66**, 014204 (2002).
- [24] Eugene Sorets and Thomas Spencer, Positive Lyapunov Exponents for Schrödinger Operators with Quasi-Periodic Potentials, *Commun. Math. Phys.* **142**, 543-566 (1991).
- [25] P. S. Davids, Lyapunov exponent and transfer-matrix spectrum of the random binary alloy, *Phys. Rev. B* **52**, 4146 (1995).
- [26] K. Ishii, Localization of eigenstates and transport phenomena in the one-dimensional disordered system, *Progr. Theor. Phys. Suppl.*, **53**: 77 (1973).
- [27] H. Furstenberg, Noncommuting random products, *Trans. Amer. Math. Soc.*, **108**: 377-428 (1963).
- [28] R. A. Johnson, Exponential dichotomy, rotation number, and linear differential operators with bounded coefficients, *J. Differential Equations* **61** (1986): 54-78.
- [29] Yongjian Wang, Xu Xia, Jiangong You, Zuohuan Zheng, and Qi Zhou, Exact mobility edges for 1D quasiperiodic models, *arXiv:2110.00962* (2021).
- [30] Stefano Longhi, Metal-insulator phase transition in a non-Hermitian Aubry-André-Harper model, *Phys. Rev. B* **100**, 125157 (2019).
- [31] Dave J. Boers, Benjamin Goedeke, Dennis Hinrichs, and Martin Holthaus, Mobility edges in bichromatic optical lattices, *Phys. Rev. A* **75**, 063404 (2007).
- [32] Xiaopeng Li, J. H. Pixley, Dong-Ling Deng, Sriram Ganeshan, and S. Das Sarma, Quantum nonergodicity and fermion localization in a system with a single-particle mobility edge, *Phys. Rev. B* **93**, 184204 (2016).

- [33] Dong-Ling Deng, Sriram Ganeshan, Xiaopeng Li, Ranjan Modak, Subroto Mukerjee, J. H. Pixley, Many-body localization in incommensurate models with a mobility edge, *Annalen der Physik*, **529**, 1600399 (2017).